# Development of a vernix caseosa substitute : a novel strategy to improve skin barrier function and repair

Rißmann, R.

# 3

# Temperature induced changes in structural and physicochemical properties of vernix caseosa

Robert Rissmann[1], Wouter Groenink[1], Gert Gooris[1], Marion Oudshoorn[2], Wim Hennink[2], Maria Ponec[1] and Joke Bouwstra[1]

[1] Department of Drug Delivery Technology, Leiden/ Amsterdam Center for Drug Research,
[2] Department of Pharmaceutics, Utrecht Institute for Pharmaceutical Sciences

Adapted from *Journal of Investigative Dermatology* 2008; 128(2):292-299

**Abstract**
The skin of the third trimester foetus and early newborn exhibits a complex, multifunctional, highly hydrated but viscous skin-surface biofilm called vernix caseosa. During birth, vernix caseosa undergoes a substantial change from an aqueous and warm surrounding into a gaseous and colder environment postnatally. The aim of this study was to investigate the structural and physicochemical changes in vernix caseosa which accompany physiologically relevant variations in environment parameters such as temperature and humidity. A remarkable difference was observed in water release and uptake properties: dehydration and rehydration processes take place 2-4 times faster at 37°C than at room temperature. The dehydration was irreversible; rehydration was only possible to a final weight of 55 % (37°C) and 46 % (room temperature) of the pre-desiccation weight. Differential scanning calorimetry showed two different overlapping phase transitions within physiological temperature range. Investigation of the lipid organization by Fourier transform infrared spectroscopy and small-angle X-ray diffraction revealed a more disordered state of lipids at 37°C than at room temperature, which might explain the faster dehydration and rehydration process at 37°C as well as the changes in thermotropic rheological behaviour. In conclusion, we demonstrated that vernix caseosa properties adjust to the fundamental change from the intrauterine to the postnatal environment.

**Introduction**
The skin constitutes the major barrier between our organism and the environment. During the development of the skin *in utero,* the skin of the fetus is often covered by a creamy, white biofilm called vernix caseosa (VC). The formation of VC commences in the beginning of the last trimester of gestation and after delivery it dries spontaneously on the skin. VC consists of detached corneocytes very similar to those of the underlying uppermost layer of the epidermis, the stratum corneum (SC). VC corneocytes are polygonal or ovoid in shape with diameters of 10-40 µm [1]. The corneocytes are embedded in a lipid matrix and thus, VC's basic structure shows similarities to that of the SC. However, VC consists of ~80 % water, ~10 % proteins and ~10 % lipids [2, 3]. The lipid fraction is mainly composed of sebaceous-derived, nonpolar lipid classes comprising squalene, sterol esters, wax esters and triglycerides [4, 5]. Recent studies revealed that the barrier lipids - cholesterol, free fatty acids and ceramides [2] - and lipids bound to the corneocytes of VC are present [6] in composition similar to that of SC. The level of barrier lipids in VC is, however, much lower than in SC. Protein analysis showed the presence of antibiotic polypeptides [7, 8] and polypeptides with innate immunity functions [9].
*In utero,* VC constitutes a unique barrier between the amniotic fluid and the skin of the fetus. It has been proposed to play an important role in barrier formation [3], SC hydration and pH-regulation in the neonatal skin adaptation process [10]: VC

increases SC hydration and in addition it seems to enhance the acid mantle development after birth. In other reports it was shown that VC acts as a skin cleanser [11] and that it has multiple protective functions such as that of moisturizer, anti-infective and antioxidant [12]. This multifunctional character of VC has been emphasized by Hoath *et al.* [13] who concisely reviewed VC characteristics.

During birth, however, VC undergoes a substantial change and is transferred from an aqueous, warm and sterile environment to a gaseous, colder and xenobiotic-containing environment in the postnatal situation. In the prenatal period, VC might facilitate skin maturation and in the postnatal period it might affect SC hydration. Therefore, changes in physicochemical properties of VC during birth are of great interest in order to better understand its role after birth. It has been reported that temperature is of importance for the yield value of VC, i.e. the minimum required shear stress to initiate flow [14]. As no additional data on temperature and hydration induced changes in VC has been reported yet, in the present study the physicochemical and structural properties of VC were investigated as function of temperature. This information will certainly contribute to a better understanding of the effect of the natural environment on the properties of VC and the role VC plays after delivery.

Dehydration and rehydration of VC were monitored at 37°C and room temperature (RT). Moreover, the localisation of water in VC during dehydration and rehydration was examined by cryo-scanning electron microscopy (Cryo-SEM). Temperature-induced phase transitions and their effect on VC properties between 15°C and 37°C were explored by means of Fourier transform infrared spectroscopy (FTIR), differential scanning calorimetry (DSC) and small-angle X-ray diffraction (SAXD). Changes in flow properties were monitored by rheological studies. These combined techniques provided insight into the structural and physicochemical changes of VC.

**Materials & Methods**

*Collection and preparation of vernix caseosa*

VC was scraped off gently with a sterile plastic spoon immediately after vaginal delivery or caesarean section of healthy term neonates. The samples were transferred in sterile plastic tubes, and stored at 4°C until use. For the experiments, various samples from different donors were used. The collection of VC was approved by the ethical committee of the Leiden University Medical Center and informed consent was given by the parents. The samples were taken in adherence to the principles of the Declaration of Helsinki.

*Dehydration and rehydration*
Weighing boats with a well-defined surface area (30 $mm^2$) and depth (1 mm) were designed in such a manner that the boats were filled with VC having a flat surface and a constant thickness. The VC samples (three donors, each with three replicates) were transferred into $P_2O_5$ containing desiccators and dehydrated at 22-24°C (RT) and at 37°C, respectively. During the dehydration process the samples were weighed (Microbalance, Mettler TG 50, Switzerland) at various time intervals. After dehydration, the samples were rehydrated at 100 % relative humidity over MilliQ water until a constant weight value was reached. In order to study reversibility of water-holding properties, the rehydrated samples were dehydrated again. Weight percentage (t=0, 100 %) was plotted against time.
In order to visualize ultrastructural changes during the dehydration and rehydration process, VC samples were also collected to examine the water distribution by cryo-SEM technique as described in more detail in a previous study [6]. Briefly, a small amount of VC (~1 mg) was placed in a small cylindrical sample holder and cryo-fixed in liquid propane (KF80, Reichert-Jung, Vienna, Austria). The cryo-fixed samples were sliced at -90°C and transferred into the cryo-scanning electron microscope (6300 FESEM, Yeol, Tokyo, Japan). The samples were freeze dried for 1 min at -90°C at 0.1 Pa and subsequently coated with 5 nm platinum. The samples were examined in the electron microscope at -190°C. With this method free water can be detected in the structure.

*Differential scanning calorimetry*
DSC analysis was performed to study the thermotropic behaviour of VC. DSC measurements were performed on a Q-1000 calorimeter (TA Instruments, New Castle, Delaware, USA). 5-10 mg of the fresh VC was transferred into an aluminium pan which was hermetically sealed in order to prevent evaporation of water. After 5min equilibration at 5°C DSC was performed with a heating rate of 2°C/min and a modulation of ±1°C/min up to 50°C. The reversibility of the events was studied by cooling and heating cycles between 5 and 50°C.

*Fourier transform infrared spectroscopy*
Fresh VC samples were sandwiched with a distinct thickness of 12 µm between two ZnSe windows. Subsequently, the windows were mounted into a special designed heating/cooling cell. FTIR spectra were acquired on a Bio-Rad Excalibur FTS 4000 XM (Bio-Rad Laboratories Inc., Cambridge, Massachusetts, USA), equipped with a SHA 10 FTIR air purifying system (Hitma BV, Uithoorn, the Netherlands) and a mercury–cadmium–telluride detector which was cooled with liquid nitrogen. The infrared spectra in the frequency range of 400-4000 $cm^{-1}$ were collected during 1 min at 2°C intervals between 10 and 50°C as a function of temperature (heating rate of 0.25°C/min). Each spectrum resulted from the co-addition of 128 scans with a nominal resolution of 1 $cm^{-1}$.

*Small-angle X-ray diffraction*

The SAXD measurements were conducted at station BM26B at the European Synchrotron Radiation Facility in Grenoble, France [15]. Fresh VC samples (~3 mg) were applied onto a mica window, transferred into a special sample holder which was subsequently mounted in the X-ray beam. The diffraction data were collected by a two-dimensional gas-filled area detector with a 1.5 m sample-detector distance. The X-ray wavelength was 1.24 Å. Sequential diffraction patterns were acquired during heating and subsequent cooling between 15°C to 35°C for 2 min/°C. Diffraction data were collected on a two-dimensional multiwire gas-filled area detector. The spatial calibration of this detector was performed using silver behenate and cholesterol.

*Rheology*

Flow properties of VC were studied on a rheometer (AR1000-N, TA instruments, Etten-Leur, The Netherlands) with a steel cone (1°, 20 mm diameter). In order to prevent the evaporation of water a solvent trap was installed above the cone. Viscosity and elasticity were recorded in the oscillation mode with a controlled strain of 0.1 % at a frequency of 1 Hz. The temperature-induced changes were studied between 10 and 45°C with a heating/cooling rate of 2°C/min.

## Results

*Irreversible water holding properties of VC during a dehydration-rehydration cycle*

Dehydration and rehydration studies of VC were performed to obtain information about the water holding properties of VC. First the dehydration rate of VC was investigated at RT and 37°C over $P_2O_5$, after which rehydration at 100 % relative humidity was also examined at both temperatures. In order to determine whether dehydration was reversible, the rehydrated samples were dehydrated again. The results of these studies are shown in figures 1 and 2. The following observations are of importance: Firstly, at 37°C dehydration of VC is characterized by a very constant water loss during the first 48 h (Fig. 1). Only in the initial hour the dehydration rate is faster (inset Fig. 1). After 72 h the dehydration process is complete, resulting in a final weight of 18.6 ± 2.5 % of the original sample. This corresponds to the composition of VC with ~10 % lipids and ~10% proteins [2, 3]. The dehydration at RT is also characterized by a constant weight loss (Fig. 1), except for the first few hours. The dehydration is complete after 240 h with a final weight of 19.8 ± 2.6 % of the original sample. The dehydration process at 37°C, however, is much faster than at RT. This is illustrated by the linear slope, which correlates to a loss of 14.7 mg water per gram VC per hour (interval from 2-48 h, $R^2$=0.99) and a loss of 3.8 mg/g/h (3-144 h, $R^2$=0.99) at 37°C and RT, respectively.

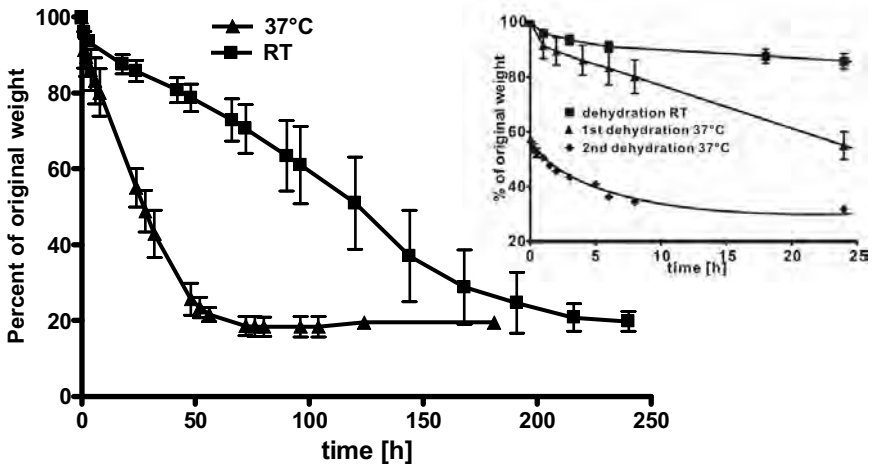


**Figure 1.** Temperature-dependent dehydration of VC. The weight percentage of VC is plotted as a function of dehydration period. VC samples (n=3) were dehydrated in a desiccator over $P_2O_5$ at room temperature (RT, squares) and 37°C (triangles) for 240 h. The first 25 h of dehydration are presented in the inset together with the dehydration after the rehydration period (diamonds). Data is presented as mean w/w ± SD%.

Secondly, rehydration is a slower process than dehydration. In figure 2A the rehydration of the VC at RT and 37°C is depicted. At both temperatures, a gradual increase in the water level in VC is observed. The water uptake was more rapid at 37°C than at RT. The entire rehydration processes at both temperatures show a hyperbolic shape: the longer rehydration takes place the slower the water uptake of VC is. In figure 2 is depicted that the rehydration rate at 37°C is approximately twice the rehydration rate observed at RT. Furthermore, comparing figure 1 and 2, it can be seen that the rehydration rate is 2 to 3 times slower than the dehydration processes. The rehydration was conducted until a constant weight of VC was obtained. In the graph (Fig. 2) this is indicated by a plateau. At 37°C the final weight with equilibrium water content of VC after de- and rehydration is 55.4 ± 3.4 % (w/w) whereas at RT the final weight is 46.0 ± 1.7 % of the initial value. This indicates that after rehydration the equilibrium water content is lower than the water content of VC prior to dehydration. This suggests that the dehydration – rehydration process is irreversible.

Thirdly, when after rehydration, a 2nd dehydration is performed at 37°C, the dehydration occurs faster than the dehydration of the original samples, as depicted in figure 1. The dehydration rate in the linear part of the second dehydration curve between 5 min and 2 h is 53.1 mg/g/h ($R^2$=0.99). This constitutes an almost 4 times higher water release rate as compared to the dehydration of fresh VC samples.

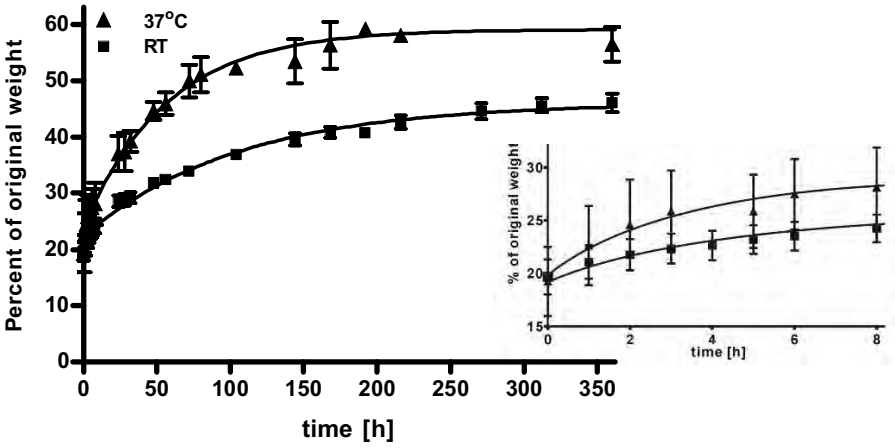


**Figure 2.** Rehydration of VC does not reach the pre-desiccation weight. Weight percentage of VC relative to predesiccation weight as a function of rehydration period over MilliQ water (n=3). The initial 8 h period of rehydration is presented in the inset. Data is presented as mean w/w ± SD%

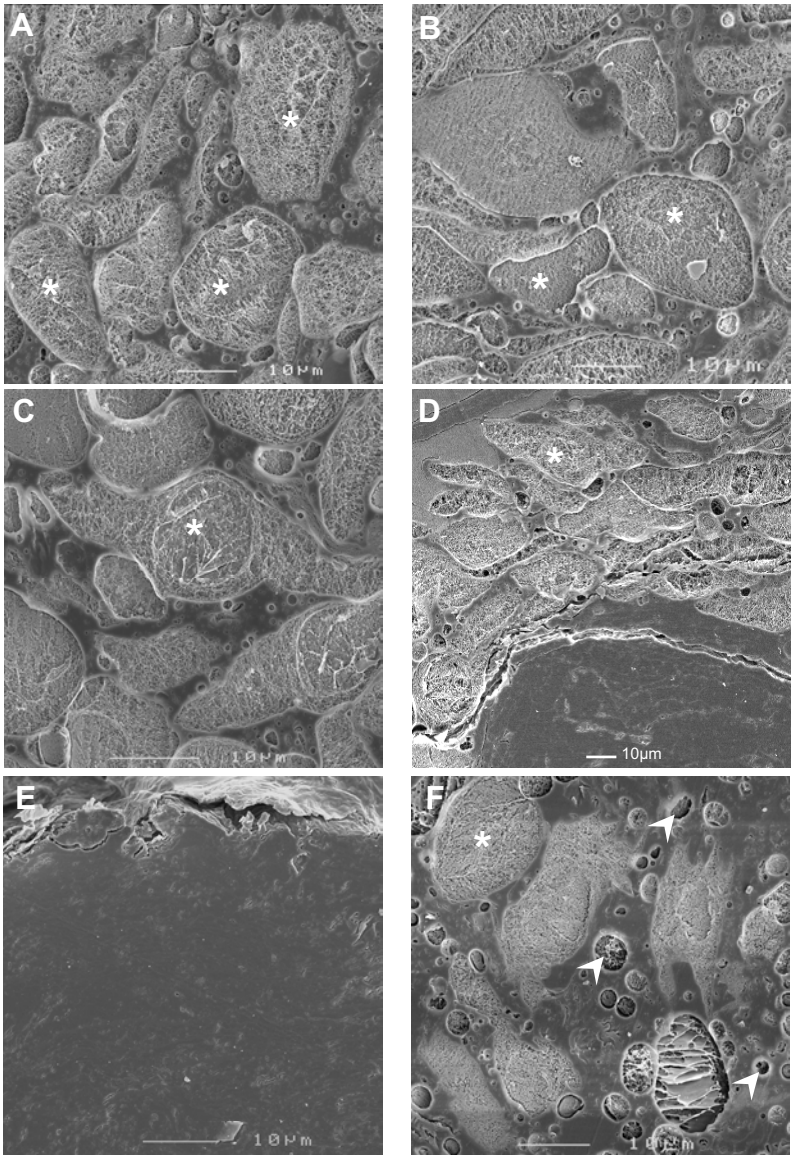


**Figure 3.** Ultrastructure of VC during the dehydration and rehydration process. VC visualized by cryo-SEM at various hydration levels expressed as weight percentage of VC relative to the predesiccation weight: 100 % (A), 71 % (B), 61 % (C), 40 % (D), 20 % (E) of original weight after dehydration and 50 % (F) of original weight after rehydration from completely dehydrated. Corneocytes (*) are characterized by dark regions (localization of water) and a white network representing keratin. These cells are embedded in the smooth appearing lipid matrix. In the lipid matrix round structures are present representing phase separated water. The number of round structures (indicated by arrow heads) increased after rehydration (F). *Scale bars* = 10 µm

*During dehydration, cryo-SEM reveals changes in the ultrastructure of VC only at low water content in VC - Rehydration results in a reduced amount of water in the corneocytes and an increasing number of water domains in the lipid domains*

In order to determine the localization of the water in VC during the dehydration process, samples were collected at various time intervals and investigated by cryo-SEM. In figures 3A-E the ultrastructure of VC samples at various dehydration states are shown. Untreated VC exhibits corneocytes in which scaffolds of dense keratin fibres are visible (asterisk in Fig. 3A). These cells are characterized by a high contrast which is caused by water (dark regions) and the keratin (white network) in the interior of the cells. The corneocytes are embedded in a matrix of the smooth appearing lipids and are hardly in contact with each other. In the lipid matrix small round structures are observed which most likely represent water droplets [6]. After partial dehydration at RT (29 % and 39 % weight loss, Fig. 3B and 3C, respectively), the corneocytes exhibit the same appearance as observed in fully hydrated VC with the water mainly localized in the corneocytes. The droplets observed in fresh VC (Fig. 3A) are visible as well. A further dehydration (60 % weight loss) yielded regions with water containing corneocytes which have almost the same appearance as at higher hydration states. They appear slightly less round in shape (Fig. 3D). In the same sample, also large domains characterized by a very smooth appearance with no contrast were observed, indicating areas where originally water was present. In fully dehydrated VC samples (80 % weight loss) the SEM photomicrographs showed only a very smooth surface (Fig. 3E), indicating the absence of water domains. After full dehydration, VC was rehydrated and subsequently studied with cryo-SEM. The appearance of rehydrated VC is very different from the fresh samples. A large number of water-filled round structures is now observed (arrowheads in Fig. 3F) within the lipid matrix. Corneocytes are also visible (*). However, the keratin filaments in the corneocytes are much more densely packed than observed in the images of the fresh VC suggesting that less water is present in the corneocytes.

*Thermotropic transitions occur in VC within physiological temperature range*

The thermotropic phase behaviour of VC was investigated by DSC between 5 and 50°C. Upon heating of VC samples, the DSC thermogram showed two overlapping peaks (Fig. 4). The exothermic transition has an onset temperature of 20.1± 0.3°C. This event was followed by an endothermic transition with an onset at 25.9± 1.4°C. Both transitions show similar enthalpies of transitions, namely -0.18± 0.1 J/g for the exothermal transition and 0.20± 0.0 J/g for the endothermal transition.

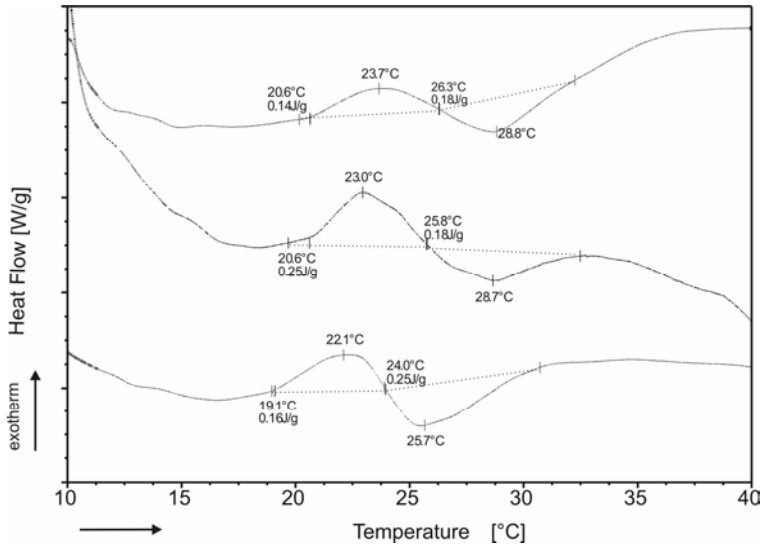


**Figure 4.** Thermotropic phase transitions of VC as observed by DSC. This method was employed to examine phase transitions in VC between 5 and 50°C. The heat flow of three different VC samples is provided as the function of temperature during the heating process.

No transitions were observed during the cooling cycle performed immediately after heating. In order to obtain information about the reversibility of the transitions, the heating and cooling cycle was followed by a 2nd heating run 20 min after cooling the sample to 5°C. No transitions were detectable. However, after 1 h equilibration at RT, heating of the sample showed the same transitions as observed with the fresh sample. This reversible nature suggests that the phase transitions originate from lipids in VC.

*Lipid organization is more disordered at elevated temperatures*

In order to obtain more details about the thermal induced phase transitions in VC, FTIR was employed. FTIR permits to study the conformational ordering and packing of the lipids in VC. In the FTIR spectrum of fresh VC samples one of the major absorption peaks can be ascribed to the asymmetric $CH_2$ stretching vibration (~2920 $cm^{-1}$). This peak provides information about the conformational order - disorder transitions, such as a crystalline-liquid phase transition [16]. The $CH_2$ scissoring mode located at ~1468 $cm^{-1}$ provides information about the packing of the lipids: a splitting of the scissoring contour indicates the presence of an orthorhombic lateral packing [17]. Therefore, the combination of the asymmetric stretching and scissoring modes provides information about the packing of the lipids in the sample.

The FTIR spectrum of VC shows that at 10°C the asymmetric $CH_2$-stretching vibration has a peak maximum at 2918.2 $cm^{-1}$, indicating a conformational ordered state of the lipids. When increasing the temperature, the peak maximum shifts gradually to 2924.0 $cm^{-1}$ at 28°C (see Fig. 5A), which indicates a gradual change of the conformational lipid order from an ordered to a more disordered state. The thermotropic response curve displays a plateau, which is reached at about 28°C (Fig. 5B). As far as the scissoring mode is concerned, at 10°C no splitting in the contour is observed at ~1468 $cm^{-1}$, which indicates that no orthorhombic lateral packing is present in VC (data not shown).

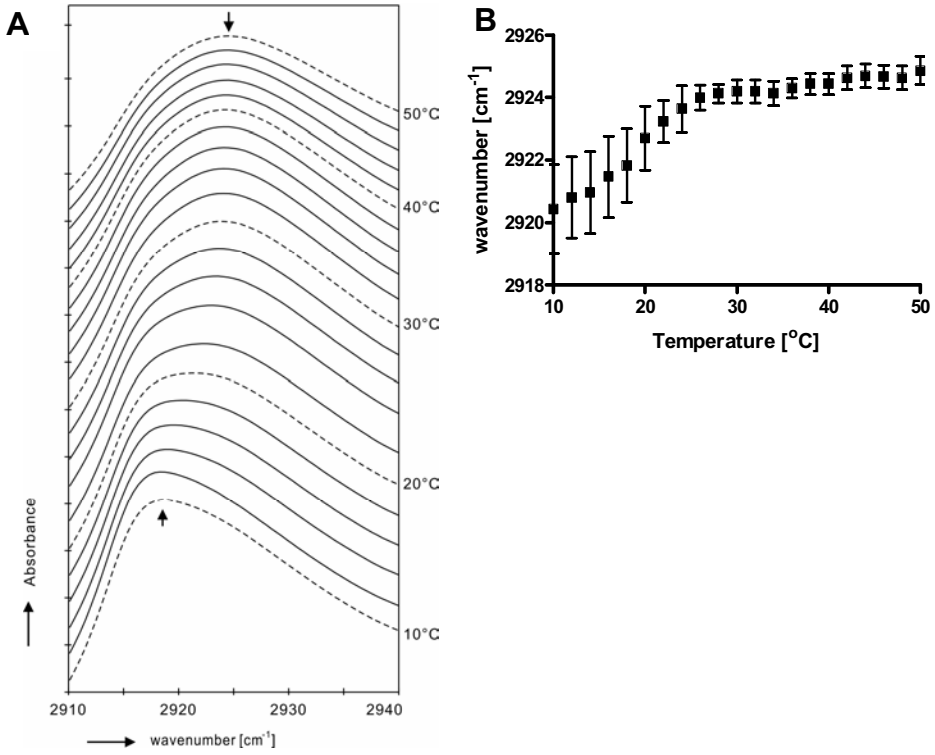


**Figure 5.** Thermotropic behaviour of VC lipids as monitored by FTIR. The FTIR spectrum of VC samples shows the asymmetric $CH_2$ stretching vibration. The spectra are depicted from 10°C to 50°C from bottom to top with 2°C interval (A). The wave number of the peak maximum of the $CH_2$ stretching vibration is plotted against the temperature in panel B. Data is presented as mean ± SD (n=3).

*Long range ordering in VC disappears at elevated temperatures, but the changes are reversible*

In our previous study, it was observed that a small population of lipids forms a long range ordering at RT, indicated by the presence of 1 or 2 diffraction peaks in the diffraction patterns of some VC samples [6]. In the present study the diffraction pattern was measured as function of temperature. A typical example is shown in figure 6. At 17°C one peak was observed at q=1.39 $nm^{-1}$ (d=4.52 nm, bottom pattern). Upon heating, the peak disappears at around 33°C indicating the absence of long range ordering in the sample. Subsequently, the sample was cooled down from 35°C (dashed pattern) to 17°C (top pattern). At around 27°C the peak at q=1.39 $nm^{-1}$ reappears which demonstrates the reversible nature of this transition.

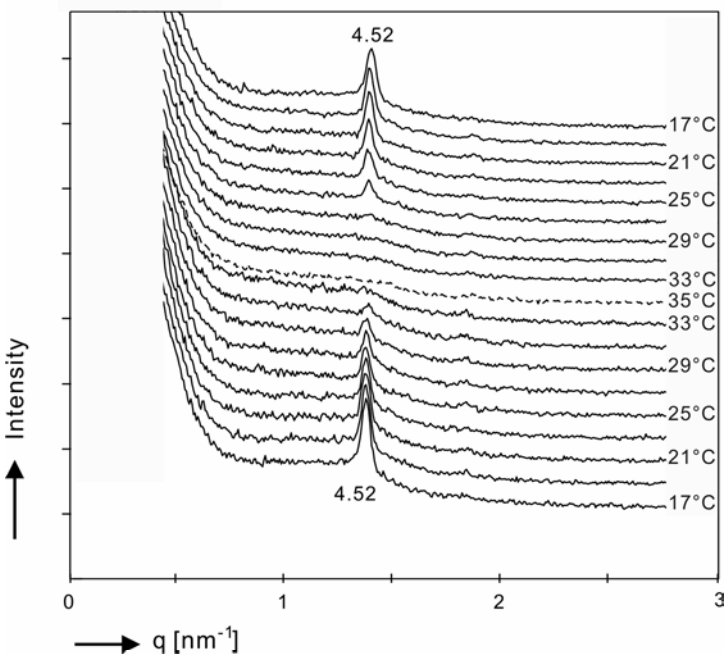


**Figure 6.** Thermotropic SAXD-patterns of VC. Scattered intensity (arbitrary units) plotted as function of scattering vector (q). Sequential SAXD patterns are plotted of a VC sample during heating from 17°C (bottom curve) to 35°C (dashed curve) and cooling down to 17°C (top curve).

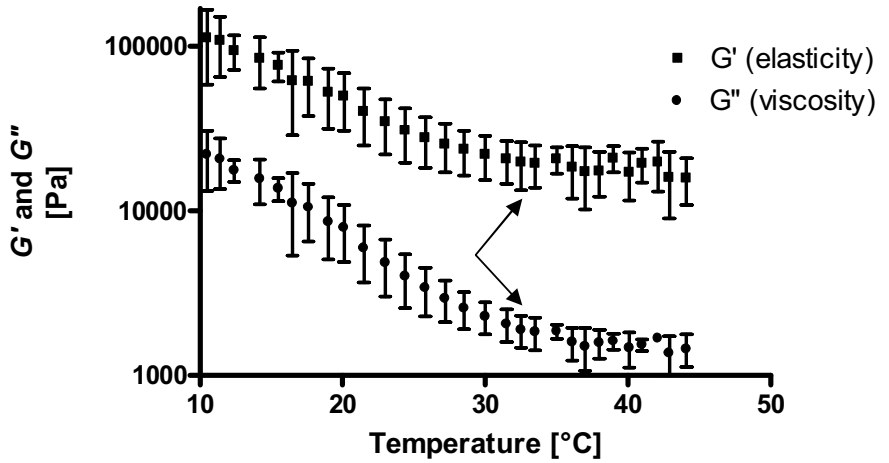


**Figure 7.** Temperature-dependent rheological characterization of VC. Rheological properties of VC were measured as a function of temperature. The shear storage modulus (G′,■) is correlated to the elasticity whereas the shear loss modulus (G″,▲) is correlated to the viscosity. Elasticity and viscosity decrease upon heating until a plateau is reached (arrows). Data is presented as mean ± SD (n=7).

*Rheological characterization of VC shows constant values for viscosity and elasticity at elevated temperatures and a reversible character*

The viscoelastic properties of VC were examined by means of rheology. Elasticity which correlates to *G′* and viscosity (correlating to *G″*) of fresh VC samples were measured as function of temperature. The results are provided in figure 7. VC showed a *tan δ*, i.e. the quotient of *G″* and *G′*, between 0.12-0.4 underlining a viscoelastic flow behaviour. The *G′* and *G″* values decline with increasing temperature and a plateau with constant values was reached at around 32°C (arrow). During the cooling process to 10°C, the viscosity and elasticity returned to the original values indicating a reversible process (data not shown).

**Discussion**

The skin of the fetus develops in an aqueous, warm and sterile environment while the SC is still premature [18]. During the intrauterine maturation of the skin barrier, VC forms an additional barrier affecting the interaction between SC and the amniotic fluid. The transition from prenatal to postnatal state marks a fundamental change in environment for the skin of the baby from aqueous surrounding at 37°C to a low relative humidity at reduced temperature. Our investigations aimed to characterize properties of VC during this transition and examine changes by biophysical and visualization methods.

*Irreversibility of water holding properties of VC*

*a. VC dehydration.*

With ~80 %, water constitutes the main component of VC [3] immediately after delivery. Being at the interface between the baby's skin (37°C) [10] and the environment (RT~22°C), VC is exposed to a substantial temperature gradient. We therefore studied the dehydration behaviour of VC at both RT and 37˚C. It can be calculated from figure 1 that at 37°C the dehydration is about 4 times faster than at 22°C. This suggests that due to a temperature gradient in VC after delivery a remarkable difference in the dehydration behaviour might occur within VC, when comparing the superficial layer of VC to the inner layer close to the baby skin. Interestingly, no ultrastructural change in VC is observed by cryo-SEM during the dehydration process, even down to 60 % of its original weight (Fig. 3C). Subsequent dehydration to 40 % of the original weight led to formation of two types of domains, namely regions with water-containing corneocytes and regions with a smooth appearance, indicating the presence of water-free domains (Fig. 3D). However, bound-water might still be present in these regions. As far as the dehydration rate is concerned, this is significantly higher in the first hour(s) of dehydration, followed by a constant weight loss in time. This decrease indicates a rapid water release in the beginning, but also a sustained release during the remaining period, the latter being substantially extended at RT. Pickens *et al.* [3] speculated that this first release might be caused by evaporation from the small round water pools, which is then followed by the constant water release from the corneocytes. Our ultrastructural investigation shows, however, that the water pools within the lipids are still present after 29 and 39 % water loss, respectively (Fig. 3B and 3C). An alternative explanation is a rapid dehydration in the initial period leading to the formation of a thin non-hydrated layer at the VC-air interface that acts as a barrier for water transport from the interior of VC. With a constant layer thickness and a constant water activity, a constant water flux (and thus a zero order decrease in weight) can be expected.

*b. VC rehydration.*

After complete dehydration, VC was rehydrated. In contrast to the finding of Pickens *et al.* [3] who submersed their specimen, a complete rehydration of VC at 100% relative humidity was not observed. Compared to the pre-desiccation weight, water levels up to around 35 % (w/w, 37°C) and 26 % (w/w, RT) were obtained, which is much lower than the original water level of about 80 % (w/w). This might be due to changes in the cornified envelope or keratin during the drying process. VC's behaviour is different from the dehydration and rehydration of SC, which is a reversible process [19]. Rehydrated VC samples revealed major ultrastructural differences in water localization and appearance

of the keratin filaments of the corneocytes (Fig. 3F) as compared to untreated VC samples (Fig. 3A): I) less water is present in the corneocytes indicating limited water uptake during rehydration; II) the presence of large number of water-filled round structures in the extracellular lipid matrix indicates that during rehydration water does not cross the densely cross-linked cornified envelope. The observed difference in water localization in rehydrated VC might also explain the increased dehydration rate from the rehydrated VC as compared to fresh VC (Fig. 1B).

*Temperature-induced changes in the VC lipid organization are reversible*

As pointed out above, the dehydration rate of VC samples at 37°C and RT is very different. Thermotropic behaviour of VC was investigated by DSC to unravel whether these differences could be related to structural changes in VC between RT and 37°C. Upon heating of VC samples two overlapping transitions were observed: an exothermic and endothermic one with onset temperatures at ~20°C and 26°C, respectively. Due to its reversible nature, these events were assigned to the changes in the organization of the intercellular lipids. In order to investigate this, the lateral packing and long range ordering in VC were examined as function of temperature with FTIR and SAXD. Combination of results from the scissoring and asymmetric stretching vibrations revealed that at RT the lipids are partially in an ordered state, but not in the orthorhombic lateral packing. Upon increasing the temperature the conformational disorder of the lipids, monitored by the asymmetric stretching mode, increased. This represents a phase change of the lipids from an ordered to disordered (liquid) state. The increase of disordering was also observed in the long range ordering of the lipids. SAXD patterns showed peaks at 4.5 nm representing the presence of lipids in a long range ordering. Upon heating the peak disappeared around 33°C (Fig. 6), which also correlates with the offset temperature of the endothermic peak measured by DSC. This transition could therefore represent a loss of the long range ordering. The reversible nature of this long range ordering was confirmed by the reappearance of the peak during the cooling of the sample. When comparing the temperature and nature of the transitions of VC with the 3 major endothermic lipid phase transitions observed in human stratum corneum [20, 21] the transitions observed in VC are very different.

*Dehydration and lipid organization*

The increased dehydration rate at 37°C can be partially ascribed to the higher vapour pressure of water at the elevated temperature. Pavlenko and Basok [22] showed that the dehydration from a technical water-in-oil emulsion is about 2

times higher at 40°C than at 20°C. Our results from VC indicate that the dehydration rate is up to 3.8 times higher at 37°C than at RT. The higher state of disorder in the lipid organization at 37°C might therefore have a substantial contribution to the increased dehydration rate and to the thermotropic changes in elasticity and viscosity (figure 7). An increase in lipid disorder was also shown to increase the diffusion rate across stratum corneum [23]. The phase changes might therefore be responsible for an improved function of VC as 'waterproofing' film during the prenatal period and might facilitate skin maturation *in utero.* After birth, a substantial temperature gradient exists between the newborn's skin and its environment. This might have a major impact on VC's function. Close to the interface VC/SC, where the temperature is still 37°C, a high water release towards the skin is possible due to the lower degree of lipid order. VC in direct contact with the environment (22°C) is characterized by a higher degree of lipid order. This might account for the reduced water release from VC to the environment. Moreover, with the higher degree of lipid order VC forms an improved barrier to xenobiotics, which may infect the neonate through the skin. Therefore, the changes in lipid organization in VC result in both a better protection of the newborn's skin and a prolongation of SC hydration. Furthermore, the decreased dehydration rate at lower temperatures is thermally advantageous to the newborn infant because evaporative water and heat loss after birth can be minimized while a flexible and hydrated skin surface mantle is retained.
For VC, the skin surface of the neonate constitutes a big challenge in terms of the tremendous temperature gradient. However, our studies show that the VC thermal transitions are of reversible nature (DSC, SAXD). This suggests that VC postnatally can undergo several transitions at the interface between skin and environment. Unlike the reversible temperature-dependent features, the water dependent properties, i.e. dehydration and rehydration, are irreversible.

In conclusion, our results clearly show I) the irreversibility of water holding properties of the VC and their ultrastructural changes and II) reversibility of the lipid organization after birth. This demonstrates the presence of temperature-dependent changes in properties of VC within the physiological temperature range, e.g. lipid organization and water holding properties. This suggests that VC adjusts to the fundamental change from the intrauterine to the postnatal environment.

## References


[1] Agorastos T, Hollweg G, Grussendorf EI, Papaloucas A. Features of vernix caseosa cells. *Am J Perinatol* 1988 Jul;5(3):253-9.

[2] Hoeger PH, Schreiner V, Klaassen IA, Enzmann CC, Friedrichs K, Bleck O. Epidermal barrier lipids in human vernix caseosa: corresponding ceramide pattern in vernix and fetal skin. *Br J Dermatol* 2002 Feb;146(2):194-201.

[3] Pickens WL, Warner RR, Boissy YL, Boissy RE, Hoath SB. Characterization of vernix caseosa: water content, morphology, and elemental analysis. *J Invest Dermatol* 2000 Nov;115(5):875-81.

[4] Haahti E, Nikkari T, Salmi AM, Laaksonen AL. Fatty acids of vernix caseosa. *Scand J Clin Lab Invest* 1961;13:70-3.

[5] Kaerkkaeinen J, Nikkari T, Ruponen S, Haahti E. Lipids Of Vernix Caseosa. *J Invest Dermatol* 1965 May;44:333-8.

[6] Rissmann R, Groenink HW, Weerheim AM, Hoath SB, Ponec M, Bouwstra JA. New insights into ultrastructure, lipid composition and organization of vernix caseosa. *J Invest Dermatol* 2006 Aug;126(8):1823-33.

[7] Akinbi HT, Narendran V, Pass AK, Markart P, Hoath SB. Host defense proteins in vernix caseosa and amniotic fluid. *Am J Obstet Gynecol* 2004 Dec;191(6):2090-6.

[8] Tollin M, Bergsson G, Kai-Larsen Y, Lengqvist J, Sjovall J, Griffiths W, Skuladottir GV, Haraldsson A, et al. Vernix caseosa as a multi-component defence system based on polypeptides, lipids and their interactions. *Cell Mol Life Sci* 2005 Oct;62(19-20):2390-9.

[9] Tollin M, Jagerbrink T, Haraldsson A, Agerberth B, Jornvall H. Proteome Analysis of Vernix Caseosa. *Pediatr Res* 2006 Aug 28;60(4).

[10] Visscher MO, Narendran V, Pickens WL, LaRuffa AA, Meinzen-Derr J, Allen K, Hoath SB. Vernix caseosa in neonatal adaptation. *J Perinatol* 2005 Jul;25(7):440-6.

[11] Moraille R, Pickens WL, Visscher MO, Hoath SB. A novel role for vernix caseosa as a skin cleanser. *Biol Neonate* 2005;87(1):8-14.

[12] Haubrich KA. Role of Vernix caseosa in the neonate: potential application in the adult population. *AACN Clin Issues* 2003 Nov;14(4):457-64.

[13] Hoath S, Pickens WL, Visscher MO. The biology of vernix caseosa. *Int J Cos S* 2006;28:319-33

[14] Narendran V, Wickett RR, Pickens WL, Hoath SB. Interaction between pulmonary surfactant and vernix: a potential mechanism for induction of amniotic fluid turbidity. *Pediatr Res* 2000 Jul;48(1):120-4.

[15] Bras W. A SAXS/WAXS beamline at the ESRF and future experiments. *J Macromol Sci Phys B* 1998;37:557-66.

[16] Mantsch HH, McElhaney RN. Phospholipid phase transitions in model and biological membranes as studied by infrared spectroscopy. *Chem Phys Lipids* 1991 Mar;57(2-3):213-26.

[17] Casal HL, Mantsch HH. Polymorphic phase behaviour of phospholipid membranes studied by infrared spectroscopy. *Biochim Biophys Acta* 1984 Dec 4;779(4):381-401.

[18] Chiou YB, Blume-Peytavi U. Stratum corneum maturation. A review of neonatal skin function. *Skin Pharmacol Physiol* 2004 Mar-Apr;17(2):57-66.

[19] Anderson RL, Cassidy JM, Hansen JR, Yellin W. Hydration of stratum corneum. *Biopolymers* 1973 Dec;12(12):2789-802.

[20] Bouwstra JA, Peschier LJC, Brussee J, Bodde HE. Effect of N-Alkyl-Azocycloheptan-2-Ones Including Azone on the Thermal-Behavior of Human Stratum-Corneum. *International Journal of Pharmaceutics* 1989 May 15;52(1):47-54.

[21] Golden GM, Guzek DB, Harris RR, McKie JE, Potts RO. Lipid thermotropic transitions in human stratum corneum. *J Invest Dermatol* 1986 Mar;86(3):255-9.

[22] Pavlenko AM, Basok BI. Kinetics of Water Evaporation from Emulsions. *Heat Transfer Research* 2005;36(5):425 - 30.

[23] Ogiso T, Ogiso H, Paku T, Iwaki M. Phase transitions of rat stratum corneum lipids by an electron paramagnetic resonance study and relationship of phase states to drug penetration. *Biochim Biophys Acta* 1996 May 31;1301(1-2):97-104.